

Modeling of enzyme-catalyzed P–O bond cleavage in the adenosine triphosphate molecule

Maria G. Khrenova,^{*a,b,c} Tatiana I. Mulashkina,^a
Roman A. Stepanyuk^{a,b,c} and Alexander V. Nemukhin^{a,c}

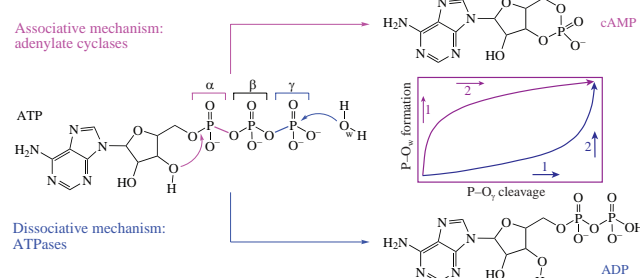
^a Department of Chemistry, M. V. Lomonosov Moscow State University,
119991 Moscow, Russian Federation. E-mail: mkhrenova@lcc.chem.msu.ru

^b Federal Research Centre 'Fundamentals of Biotechnology' of the Russian Academy
of Sciences, 119071 Moscow, Russian Federation

^c N. M. Emanuel Institute of Biochemical Physics, Russian Academy of Sciences,
119334 Moscow, Russian Federation

DOI: 10.1016/j.mencom.2024.01.001

Recent achievements in molecular modeling of reaction mechanisms of the enzymatic ATP conversion to ADP or cAMP are discussed. Both of these reactions are initiated by the nucleophilic attack of an oxygen atom, but the P–O bridging bond cleavage occurs *via* different mechanisms, dissociative and associative. These mechanisms differ in the order of formation and cleavage of P–O bonds. For ATPases, the dissociative mechanism is assumed, whereas ATP conversion to the cAMP occurs *via* associative mechanism. We suggest a novel approach based on the molecular dynamics simulations with combined quantum mechanics/molecular mechanics potentials of the enzyme–substrate complexes that can discriminate dissociative and associative reaction pathways by analysis of length distributions of the cleaving and forming P–O bonds.



Keywords: ATP, ATPase, adenylate cyclases, dissociative mechanism, associative mechanism, molecular dynamics, QM/MM.

Plenty of biologically active molecules are crucial actors in various cellular processes; however, a molecule of adenosine triphosphate (ATP) is on the ear of everyone who is even slightly familiar with the basics of biochemistry. Scholars know that this

compound is an important component of cellular metabolism and energy storage, and chemical reactions of its triphosphate entity drive a diverse range of principal molecular mechanisms in cells.^{1,2}



Maria G. Khrenova is a Professor at the Department of Chemistry of the Lomonosov Moscow State University and a Head of the Group of Molecular Modeling at the Federal Research Centre of Biotechnology of the Russian Academy of Sciences. The area of her scientific interest is molecular modeling including computational and quantum chemistry and its application to the study of reaction mechanisms in biochemical systems.



Tatiana I. Mulashkina is a postgraduate student of the Laboratory of Quantum Chemistry and Molecular Modeling at the Chemistry Department of the Lomonosov Moscow State University. The area of her scientific interest is molecular modeling of dynamic processes in biological systems and mechanisms of enzymatic reactions.



Roman A. Stepanyuk is a postgraduate student of the Laboratory of Quantum Chemistry and Molecular Modeling at the Chemistry Department of the Lomonosov Moscow State University and a junior researcher at the Group of Molecular Modeling of the Federal Research Centre of Biotechnology of the Russian Academy of Sciences. The area of his scientific interest is the computational chemistry, molecular modeling and computer-aided drug design.



Alexander V. Nemukhin[†] (1946–2023) was a Professor at the Department of Chemistry of the Lomonosov Moscow State University and a Head of the Laboratory of Computation Modeling of Biological Systems at the Emanuel Institute of Biochemical Physics of the Russian Academy of Sciences. The area of his scientific interest was modeling of dynamic processes in biological systems and mechanisms of enzymatic reactions.

[†] Deceased.

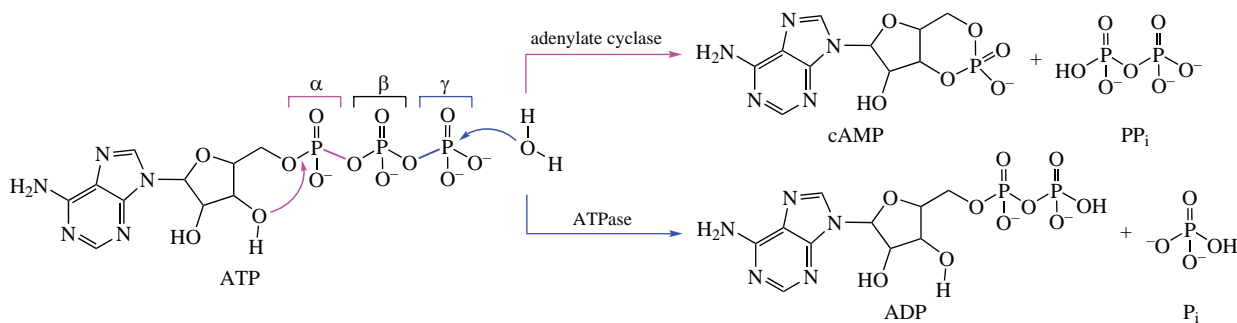


Figure 1 Chemical transformations of the ATP: ATP conversion to the cAMP and PP_i in the active site of adenylate cyclases and ATP hydrolysis to ADP and P_i by ATPases.

When consumed in metabolic processes ATP loses either one or two of three phosphate groups converting to adenosine diphosphate (ADP), or adenosine monophosphate (AMP), respectively. The corresponding chemical reactions catalyzed by specific enzymes have been in the focus of numerous studies aiming to determine elementary steps and thus to establish reaction mechanisms. It is hard to overestimate the significance of experimental investigations; however, computer simulations provide an essential contribution in this field. For years, various models were proposed to explain reactions of enzyme-catalyzed release of the phosphate groups from the ATP in different protein environments. It should be noted that the major efforts were directed towards the hydrolysis reaction involving cleavage of the P–O bond at the terminal phosphate group and formation of ADP since this reaction is at the heart of bioenergetics. Enzyme-catalyzed release of diphosphate from ATP was also modeled with the relevance to intracellular signaling. Chemical transformations during these reactions are depicted in Figure 1. Those are ATP conversion to the adenosine diphosphate (ADP) and phosphate (P_i) and ATP conversion to the cyclic adenosine monophosphate (cAMP) and pyrophosphate (PP_i). The first reaction is catalyzed by ATPases and the second – by adenylate cyclases. Formally, both of these reactions are initiated by the nucleophilic attack of phosphorus atom leading to the cleavage of the bridging P–O bond. The details of reaction mechanisms are still actively discussed from both experimental and theoretical aspects.³

Historically, quantum-based simulations of ATP transformations in proteins and solutions started from simple molecular models described at the quantum chemistry level. Formulation and practical implementation of the quantum mechanics/molecular mechanics (QM/MM) theory provided a dramatic breakthrough in enzyme catalysis, in particular, in the ATP chemistry. Analysis of the computed energy profiles as the minimum energy pathways connecting reactants and products allowed researchers to propose detailed reaction mechanisms of ATP transformations. A modern era started when direct calculations of the free-energy reaction profiles become available from molecular dynamics simulations with the QM/MM interaction potentials. These approaches will be discussed in details below.

Due to a high importance of the P–O bond cleavage both in the enzymatic reactions and in solutions, the classification of the mechanisms is proposed. During the reaction, the covalent bond between the phosphorus atom and the nucleophile, P–Nu, is formed and the covalent bond between the phosphorus atom and the leaving group, P–L, is cleaved (Figure 2). The reaction can follow associative or dissociative mechanism *via* intermediate state or a single step. A more detailed description can be found in ref. 3.

The goal of this paper is to review the most essential findings on ATP decomposition as revealed in quantum-based simulations.

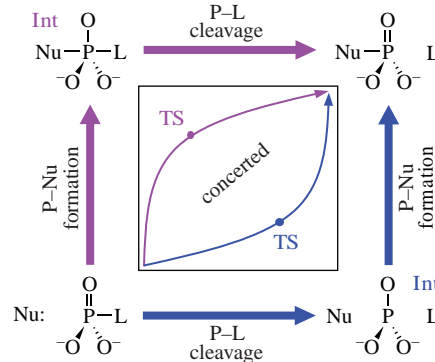
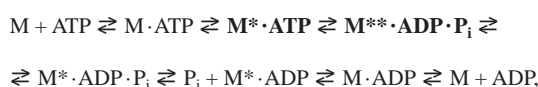


Figure 2 Mechanisms of the P–O bond cleavage. A nucleophile, Nu:, attacks a phosphorus atom, P, and a leaving group, L, is released. Reaction can occur *via* two steps with an intermediate, Int, or in a single step, concerted mechanism. In the associative mechanism, formation of the P–Nu bond precedes the P–L bond cleavage (magenta). In the dissociative mechanism, the P–L bond is cleaved first and then the P–Nu bond is formed (blue).

From the chemical perspective, it is important that reactions leading to the ADP or cAMP (see Figure 1) follow different mechanisms (see Figure 2), and this conclusion can be rationalized irrespective of the applied computational protocols. Moreover, this can be rationalized by computational analysis of the dynamic features of enzyme–substrate complexes that we present in the last part of this focus article.

ATP conversion to ADP and P_i Myosin

Myosin is a motor protein that plays a key role in converting chemical energy of ATP hydrolysis into mechanical energy for muscle contraction.⁴ In 1974, a seven step kinetic scheme of the process of binding and hydrolysis of ATP by myosin was proposed:⁵



where M is myosin and asterisks indicate different conformations of the protein. The chemical step of process is highlighted bold in the scheme and it is characterized by the equilibrium constant that almost equals unity. Rate constants for the forward, k_+ , and backward, k_- , reactions are $k_+ \geq 160 \text{ s}^{-1}$ and $k_- \geq 18 \text{ s}^{-1}$, respectively.^{5,6} This corresponds to the energy barrier of the forward reaction $\Delta G^\ddagger = 14.6 \text{ kcal mol}^{-1}$ at 300 K according to the transition state theory. This value is related to the limiting step and might be attributed to either chemical reaction itself or to the related conformational changes of the protein. Also, ^{31}P NMR data and ^1H diffusion measurements evaluate activation energy to be $10.3 \text{ kcal mol}^{-1}$ according to the Arrhenius relation and measurements in $21\text{--}50^\circ\text{C}$ temperature range.⁷

The more detailed information on the ATP hydrolysis reaction mechanism can be obtained from molecular modeling.^{8–16} Earlier studies were performed for small isolated molecular clusters and did not account for the protein surrounding.⁸ In this model, the lytic water molecule was located between the Arg238 and Glu459 ‘gates’ and γ -phosphate group of the ATP. The distance of the nucleophilic attack was 3.41 Å in the reactant state and decreased to 2.17 Å in the transition state. Upon reaction, the covalent bond between oxygen atom of a water molecule and phosphorus is formed and one of the protons of the hydrogen atom is transferred to the oxygen atom of the γ -phosphate group. These calculations were performed at the HF/6-31G** level and the calculated energy barrier was 58.6 kcal mol^{–1}. Recalculation of the stationary point energies results gives only 16.7 kcal mol^{–1} decrease of the energy barrier. The following calculations were performed with taking into account the influence of the protein environment on the active site.^{9–16}

Li *et al.*⁹ compared two associative mechanisms using QM(B3LYP/6-31G**+)/MM(CHARMM)//QM(HF/3-21G+)/MM(CHARMM) approaches that differed in the way of the proton transfer from the lytic water molecule to the oxygen atom of the γ -phosphate group. It was proposed that the proton might be transferred either directly or *via* hydrogen bond network comprising Ser236. The latter way was \sim 4 kcal mol^{–1} energetically more favorable, but still, all energy barriers exceeded 20 kcal mol^{–1}. Similar calculations were performed by Schwarzl *et al.*¹⁰ and they also extended the set of possible pathways adding the proton transfer through the hydrogen bond network with Ser181 residue. Similarly, energy barriers were higher than 20 kcal mol^{–1} and strongly depended on the QM protocol. The mechanism comprising Ser236 in the proton transfer was also studied using SCC-DFTBPR to describe QM part in the QM/MM simulations.¹¹ This theory level was chosen to be able to calculate MD trajectories with QM/MM potentials. The energy barrier calculated for the potential of mean force (PMF) was 16 kcal mol^{–1} that is close to the experimental value. Still, it is known that DFTB is not a reliable computational protocol for calculations of chemical reactions in the active site of enzymes and these results should be carefully checked by other methods.^{17,18}

Later, Onishi *et al.* analyzed available X-ray data and proposed a reaction mechanism called ‘two-water’ hypothesis.^{19,20} According to this mechanism, one water molecule is lytic and it performs hydrolysis reaction, whereas the second one acts as a proton acceptor. During the reaction, the second water molecule transforms to the positively charged H₃O⁺ and is stabilized by negatively charged carboxylate of the Glu470 side chain and the backbone carbonyl of the Gly468.

The ‘two-water’ hypothesis was further developed in computational studies.^{12–16} Grigorenko *et al.* compared ‘one-water’ and ‘two-water’ mechanisms^{12,13} at the QM/MM level. Authors utilized two different hybrid DFT functionals in the QM subsystem and obtained consistent results for energy barrier: 8.1 and 10.4 kcal mol^{–1} for B3LYP and BB1K functionals, respectively. According to this mechanism, a proton from the lytic water molecule is transferred to the Glu459 carboxylate *via* hydrogen bond network formed by the second water molecule. The energy barrier calculated for model system with one water molecule in the active site was 34 kcal mol^{–1}.

Kiani *et al.* analyzed different pathways of the proton transfer in the ‘two-water’ mechanism.^{14–16} They concluded that the proton wire might include Ser181 leading to the double-protonated phosphate, H₂PO₄[–]. In this mechanism, the reaction products are -2.3 ± 0.7 kcal mol^{–1} relative to the reagents, that is consistent with the experimental values -1.5 to

-2.6 kcal mol^{–1}.²¹ Still, authors suppose that other proton wires can also exist. Reaction mechanisms suggested by both Kiani *et al.*^{14–16} and Grigorenko *et al.*^{12,13} assume the dissociative pathway.

The main conclusions on the reaction mechanism of the ATP hydrolysis by myosin are as follows: (i) the reaction is likely to occur *via* ‘two-water’ mechanism; (ii) the reaction is likely to occur *via* dissociative mechanism.

F1-ATPase

ATP is mostly synthesized by F₁F₀-ATP synthase in living organisms. Part of the F₁ enzyme can also perform backward reaction, ATP synthesis.²² F1-ATPase is a rotational motor protein that works due to ATP hydrolysis and converts the energy generated during ATP hydrolysis into mechanical energy. Three ATP binding sites in the F₁-ATPase are characterized by different ATP binding affinities. The crystal structure of the F₁-ATPase shows three different active sites that might hydrolyze ATP.²³ These active sites possess different conformations called β_{TP} , β_{DP} , β_E . Abrahams *et al.* suggested that the β_{DP} site should be the most reactive according to its geometry features. Therefore, from the computational viewpoint, there are two problems to be solved: determination of the reaction mechanism and discrimination of the most preferable catalytic site.

Dittrich *et al.*^{24–26} performed QM/MM simulations and compared ATP hydrolysis reaction mechanisms in catalytic sites β_{TP} and β_{DP} . The β_{TP} catalytic center carries five water molecules, therefore different hydrolysis mechanisms might be suggested. Among them, ‘one-water’ and ‘two-water’ mechanisms can be discriminated. In ‘one-water’ mechanism, the water attacks phosphorus atom of the γ -phosphate group and the proton transfer occurs directly from the water molecule to the oxygen atom of the γ -phosphate group. A ‘two-water’ mechanism presumes a lytic water molecule that lies on the same line with the cleaving P–O bond of the ATP. In this mechanism, the proton is transferred from the lytic water to another water molecule. Still, calculated energy barriers are much larger²⁴ than that expected from the measured rate constants of $\sim 5 \times 10^{-2}$ s^{–1} for both forward and backward chemical reactions.²⁷ It was demonstrated that equilibrium constant of $K \sim 10^{-27}$ for the chemical step is more consistent with ATP hydrolysis in the β_{DP} catalytic center.²⁵

Hayashi *et al.*²⁸ performed QM/MM simulations with the experimental single molecule studies of the ATP hydrolysis in the β_{DP} catalytic site. They stated that the hydrolysis included dissociation of the P–O bond, proton transfer and a hydrogen bond network rearrangement. In the first step, the water molecules of the active site and hydrogen bond rearrangements take place. It leads to a proper orientation of the lytic water molecule. This state is about 1 kcal mol^{–1} higher in energy than the reactant state. The chemical reaction is initiated by the elementary step comprising cleavage of the P–O bond with the corresponding distance in the intermediate state of 2.68 Å. The activation energy of this step is 14.7 kcal mol^{–1}, whereas the following intermediate is only 0.2 kcal mol^{–1} lower in energy relative to the transition state. The next step is the covalent bond formation between the phosphorus atom and the γ -phosphate group and the lytic water molecule that happens with the energy barrier of 2.4 kcal mol^{–1}. This process is accompanied by the proton transfer from the lytic water molecule to the β Glu188 *via* proton wire comprising another water molecule in the active site. Such intermediate is also highly destabilized relative to the reactant being 13.1 kcal mol^{–1} higher in energy. During the following reaction steps, the proton from the β Glu188 is transferred to the oxygen atom of the P_i. The reaction products are 1.6 kcal mol^{–1} stabilized

relative to the reactant that is in agreement with the experimental equilibrium constant close to unity, 2.9.^{27,29}

Martín-García *et al.* also studied a ‘two-water’ mechanism of the ATP hydrolysis.³⁰ It was shown that the terminal proton acceptor from the lytic water molecule is an oxygen atom of the γ -phosphate group and the proton transfer occurs *via* the second water molecule of the active site. The role of the β Glu188 was explicitly demonstrated by comparison of the energy profiles with those of the wild type enzyme and the β Glu188Ala variant. This amino acid substitution leads to the increase of energy barrier from 22 to 42 kcal mol⁻¹. Authors concluded that the carboxylate of the β Glu188 residue stabilized hydronium cation during the reaction.

By now, computational studies did not arrive to the completely consistent reaction mechanism that explained all available experimental data. All considered reaction pathways are characterized by the energy barriers considerably higher than those observed in experiments. The β_{DP} catalytic site is more likely to perform ATP hydrolysis due to the stabilization of the transition state by α Arg373 and H_3O^+ formed during the reaction by β Glu188. The ‘two-water’ mechanism is more preferable, similarly to the reaction in myosin.

Kinesin

Kinesin is a motor protein that utilizes energy of the ATP hydrolysis for the cellular processes such as mitosis, meiosis and vesicle transport.³¹ Cochran *et al.* determined the rate constant of the chemical step of the reaction as 1.14 ± 0.05 s⁻¹ that corresponded to the energy barrier of 17.5 kcal mol⁻¹ according to the transition state theory.^{32,33}

McGrath *et al.* studied four different reaction pathways using metadynamics with QM/MM potentials.³⁴ The most probable is a ‘two-water’ mechanism which assumes nucleophilic attack by a lytic water molecule, the proton transfer to the Glu270 *via* the second water molecule and the proton transfer from Glu270 to the oxygen atom of the γ -phosphate. The calculated energy barrier is 11 ± 3 kcal mol⁻¹ that is considerably lower than the experimental value, and the authors conclude that it can be due to the errors of utilization of the GGA functional BLYP to calculate energies and forces in the QM subsystem. They also conclude that the suggested mechanism shares common features with hydrolysis in other motor ATPases, myosin and F₁-ATPase.³⁴

Actin

Actin is a protein involved in muscle contraction, cellular motility and division (cytokinesis), vesicle transport, as well as in the establishment and maintenance of cellular morphology.³⁵ Actin has two forms: globular monomeric actin (G-actin) and polymerized form (F-actin).

Akola *et al.* modeled four different reaction pathways in the G-actin to discriminate the most probable one.³⁶ QM/MM simulations were performed with the GGA functional PBE and plane wave basis set. It was demonstrated that the most probable is the dissociative mechanism with the energy barrier of 21 kcal mol⁻¹. According to this mechanism, the P–O of the ATP is cleaved upon shortening of the distance of the nucleophilic attack and deprotonation of the lytic water molecule. In the end of the reaction, the excess proton is located on the Asp154 and the inorganic phosphate is presented in the HPO₄²⁻ state. It is shown that the H₂PO₄⁻ state is energetically more favorable, but it can be formed along the other reaction pathway characterized by the higher energy barrier of 28 kcal mol⁻¹.

A similar mechanism was proposed by Friedman *et al.*,³⁷ based on the data obtained in minimum energy path (MEP),

nudged elastic band (NEB) and *ab initio* molecular dynamics (AIMD). The phosphorus is prepared for the nucleophilic attack of the water molecule after elongation of the covalent bond between phosphorus atom of the γ -phosphate group and bridging oxygen atom. The excess proton is transferred through two neighboring water molecules to Asp154. At the last step, a proton is transferred from the Asp154 to the phosphate P_i turning it to the H₂PO₄⁻ protonation state.

The QM/MM metadynamics simulations were performed to compare ATP hydrolysis mechanisms in G- and F-actin.³⁸ Authors claim that hydrolysis in G- and F-actin occurs by a concerted mechanism in which γ -phosphate dissociates simultaneously with the addition of lytic water. Free energy profiles demonstrate the difference of energy barriers for the hydrolysis reaction by G-actin (30 kcal mol⁻¹) and F-actin (22 kcal mol⁻¹), which is consistent with experimental data. According to the kinetic measurements, the rate of ATP hydrolysis is 0.3 ± 0.1 s⁻¹ in F-actin and 7×10^{-6} s⁻¹ in G-actin.^{39,40} The difference of rate constants corresponds to 7 kcal mol⁻¹ difference in the energy barrier at 310 K, that is practically the same as the computational estimates of 8 kcal mol⁻¹.

It was shown that the proton transfer occurs differently in the G- and F-actin, namely, proton transfer from lytic water to γ -phosphate occurs almost instantly in the F-actin, in contrast to proton transfer in the G-actin. Authors attribute the difference of energy barriers to the rearrangement of water molecules during polymerization, which leads to the formation of shorter hydrogen bonds in F-actin that facilitates a proton transfer from Asp154 residue to the phosphate.

In a recent study,⁴¹ the four-step mechanism of ATP hydrolysis by F-actin was suggested. At the first step, the rearrangement of water molecules proceeds. At the second step, the P–O bond of the ATP is cleaved and the water molecule comes closer to the phosphate. The first two stages occur with low energy barriers (about 5 kcal mol⁻¹). At the third step, several events occur simultaneously: deprotonation of the lytic water molecule, nucleophilic attack of the phosphorus atom by the hydroxide anion, proton transfer to the HPO₄²⁻ *via* another water molecule and formation of the H₂PO₄⁻. The calculated activation energy is 13–17 kcal mol⁻¹ that is in agreement with the rate constant 0.3 s⁻¹ (18 kcal mol⁻¹ according to the transition state theory).⁴⁰ At the final step, hydrogen bond network rearrangement takes place with a low energy barrier.

Thus, similar general features of the ATP hydrolysis are observed in different ATPases as demonstrated by molecular modeling methods. First, the ‘two-water’ mechanism is more preferable and at least two water molecules should participate in chemical reaction. Next, the reaction occurs according to the dissociative mechanism. Finally, the important and the most controversial step of hydrolysis is the transfer pathway of an excess proton.

Adenylate cyclases

Adenylate cyclases can be divided into two groups: transmembrane AC (tmAC) represented by nine isoforms and soluble adenylate cyclases (sAC).^{42–45} The second messenger cAMP is known for about half a century, but the experimental study of the mechanism of its formation began recently.⁴⁶ Many infectious microorganisms secrete virulence factors that increase cAMP levels in infected host cells, thereby disrupting intracellular signaling pathways.

Edema factor

One of the most studied adenylate cyclase toxins is an edema factor (EF). This family of toxins does not share structural

homology with mammalian adenylate cyclases, but catalyzes the same chemical reaction of the ATP to cAMP conversion. The mechanism of reaction of ATP conversion in the active site of EF was studied using the empirical valence bond method of quantum mechanics/molecular mechanics (QM/MM) for the first time in 2013 by Mones *et al.*⁴⁷ The calculation was carried out for two possible reaction mechanisms that differ in the stage of proton transfer. The proton acceptor was either a histidine residue or a water molecule. The energy barriers were estimated as 30 and 12–14 kcal mol^{−1}, respectively. The last of them agrees with the kinetic data.⁴⁴

Mammalian adenylate cyclases

Hahn *et al.* were among the pioneers of the studies of reaction mechanism in the active site of the mammalian adenylate cyclases (mAC).⁴⁸ Authors described computationally the reaction mechanism of ATP to cAMP conversion in mammalian AC domains C(1):C(2) of types V and II, respectively. This protein model was taken from the crystal structure PDB ID 1CJK⁴⁴ and a full-atom model system including ATP restored from its analogue ATP α S-Rp, two magnesium ions and water molecules was prepared. The QM(M06/6-31G^{*})/PCM level of theory was utilized to restore the energy profile. The authors suggested 13 possible reaction ways with the most probable one characterized by five elementary steps grouped into the proton transfer, conformational change, and phosphoryl transfer steps. The proton transfer route was represented by a specific proton wire from the OH ribose group *via* a shuttling water molecule to the nonbridging oxygen of the γ -phosphate of ATP. The free energy profile was estimated by correcting energies at stationary points on the potential energy surface by entropy contributions. Limiting step is the phosphoryl transfer with a barrier of 17.9 kcal mol^{−1}, which is generally consistent with the kinetic data.⁴³

This paper also discusses the specific displacements of atoms in various reaction paths, but it is especially interesting to note the statements about the sensitivity of the activation energy and the reaction energy as a whole to the configuration of the active center. The authors estimated the potential energy gradients relative to the shift of C α atoms to the center of mass in the states of reactants, transition complex, and products. For example, it has been shown that a shift of C α Ile397 to the center of mass by 0.23 Å leads to the reduction of the calculated activation energy from 17.9 to 15.3 kcal mol^{−1}, obtained from the kinetics of the enzyme.⁴³ This also reduces the calculated free energy difference between reactants and products associated with the enzyme from 3 to 0.24 kcal mol^{−1} compared to −1.0 kcal mol^{−1} derived from enzyme kinetics.⁴³ Also, the displacement of the C α of the Ser1028 atom to the center of mass by 0.324 Å in the transition state of the last step would further optimize the ribose conformation and thus reduce the activation energy to 15.3 kcal mol^{−1}, while the displacement of C α Arg1029, which is important for the conformation of phosphates, from the center of mass by 0.3 Å in the transition state of the last step, but not in reactants, reduces the activation energy by 1.8 kcal mol^{−1}. Thus, when modeling reaction profiles, the problem of obtaining energy barriers comparable with experiment may depend both on the error in the positions of atoms of crystal structures relative to real systems, and on the difficulty of achieving real reaction configurations of the active center relative to the initial crystal structures.⁴⁸

Jara and Martinez also contributed to the reaction mechanism studies.⁴⁹ They performed molecular dynamics simulations with classical and QM/MM potentials. The semiempirical density functional tight-binding method with the self-consistent charge approach (SCC-DFTB) was applied in QM/MM simulations.

Then obtained energy profiles were corrected in single-point DFT calculations using the B3LYP and M06 functionals. They compared reaction mechanisms in two adenylate cyclases, mAC and EF. For the latter one, two possible compositions of the active sites were assumed, with one or two magnesium cations. All energy profiles are consistent with a one-step mechanism with a pentacoordinated phosphorus in the transition states, showing features of the associative mechanism. Still, the energy barriers obtained are much higher than the experimental estimates. Authors conclude that these differences are due to the inaccuracy of the SCC-DFTB approach. The work also found that ATP exhibits different flexibility depending on the crystallographic model used. From the analysis of transition state flexibility in EF and mAC, it is shown that the transition state structure exhibits more conformational flexibility in EF than in mAC, especially in the ribose and phosphate groups. This is primarily due to the limited mobility of the ribose oxygen coordinated with Mg²⁺ ion.

In 2020, an attempt to clarify the previously proposed controversial mechanisms for the conversion of ATP to cAMP was made.⁵⁰ The same crystal structure was utilized for modeling. A more transparent protocol was utilized, implying molecular dynamics, QM/MM optimization using the Kohn–Sham DFT method with the PBE0 functional with a D3 dispersion correction and the 6-31G^{*} basis set. Authors extended the results of the previous two works. They obtained a set of four ES complexes (ES_A, ES_B, ES_C, ES_D) mainly differing in the local surrounding of the ribose OH group. In most stable ES complex (ES_A) the distance of the nucleophilic attack is 3.1 Å and the hydrogen atom of the catalytic OH group is oriented to the water molecule acting as a proton shuttle to the Asp440 residue. The ATP to cAMP conversion occurs as a single step (concerted mechanism) from the ES_A *via* associative pathway, that is both cleaving and forming P–O bonds are about 2 Å in the transition state. According to this mechanism, the energy barrier is 15 kcal mol^{−1} and the products are 2 kcal mol^{−1} stabilized relative to the ES. Three other ES complexes are considerably higher in energy than the discussed one. In one of them (ES_B), the distance of the nucleophilic attack is almost 5 Å, therefore it is senseless to calculate energy profile. In the third one, ES_C, the proton from the nucleophilic OH group should transfer to the β -phosphate *via* auxiliary water molecule. This reaction pathway was found to occur with the energy barrier of about 27 kcal mol^{−1}, which practically means that this pathway cannot be realized. The last one, ES_D, is most likely the crystal structure and shares the same features, cross coordination of magnesium cations by Asp396 and Asp440 residues. Also, it is similar to the reactive conformation proposed by Hahn *et al.*⁴⁸ Still, the energy profile estimates derived to high energy barriers. Thus, the reaction can hardly occur from the ES_D, as both energy barriers are high and this ES is energetically unfavorable itself.

Bacterial adenylate cyclases

Khrenova *et al.* published a study of the features of the conversion of ATP in the active center of bacterial light-regulated adenylate cyclase, bPAC, which can be in a dark (DS) or light (LS) state.⁵¹ The active site has two hexacoordinate magnesium cations, ATP, and side chains of nearby key residues such as glutamate and aspartate. The QM subsystem was described at the ω B97X-D3/6-31G^{**} Kohn–Sham DFT level. The MM part of the system was described with the CHARMM36 force field parameters. Classical and QM/MM molecular dynamic simulations were carried out to study the reaction mechanism. Authors discriminate differences in the active site composition of the adenylate cyclase in the dark and light states and explained

the reaction acceleration upon light irradiation. In both active sites the reaction occurs in a single step *via* associative mechanism and the proton from the glycoside OH group is transferred to the glutamate *via* water molecule.

To conclude, the ATP to cAMP conversion likely occurs in a single step *via* associative type transition state. Additional water molecule is required to transfer a proton from a nucleophile to the proton acceptor.

Reaction mechanism from the analysis of the enzyme–substrate complex dynamics

QM/MM molecular dynamic simulations with reliable methods of QM part description allow us to get a lot of information regarding the following reaction mechanism. This was already shown for hydrolysis reactions by phosphotriesterases⁵² and proteases^{53–55} and GTPases⁵⁶ and bPAC.⁵¹ Herein, we performed molecular dynamics simulations with the QM(ωB97x-D3/6-31G**)/MM(CHARMM) potentials for two systems discussed in this article, bPAC and myosin with the ATP in the enzyme–substrate complex state. The model system of the bPAC–ATP complex was taken from ref. 51, whereas the myosin–ATP complex was constructed from the PDB ID: 1VOM⁵⁷ and simulations were performed similarly to that in ref. 51. The 10 ps QM/MM molecular dynamics trajectories were calculated for both systems and distributions of the P–O distances of the nucleophilic attack and cleaving bond were analyzed (Figure 3). The distance of the nucleophilic attack is considerably larger in the bPAC than in the myosin being 3.22 ± 0.15 and 2.87 ± 0.15 Å, whereas the distribution widths are similar. Contrary, the cleaving P–O bond length in the ATP is shorter in the bPAC than in the myosin being 1.64 ± 0.03 and 1.77 ± 0.05 Å. The shorter mean value corresponds to the stronger covalent bond that presumes following associative type of mechanism. Moreover, the standard deviation for the P–O bond length of the ATP in myosin is almost twice larger than that in bPAC indicating that in the ATP this bond is more flexible and prepared for the reaction. By now, this is the only example of such comparison of the active site behavior in the systems with the associative and dissociative mechanisms of the P–O bond cleavage in the ATP. The systematic analysis of the enzyme substrate complexes of the ATP with ATPases and adenylate cyclases are required.

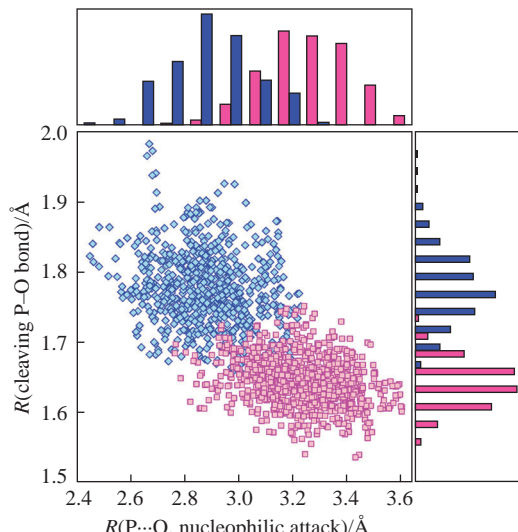


Figure 3 Distribution of P–O distances of the nucleophilic attack and cleaving bond in the myosin–ATP (blue diamonds and bars) and bPAC–ATP (magenta squares and bars) enzyme–substrate complexes obtained at the QM(ωB97x-D3/6-31G**)/MM(CHARMM) level.

Conclusion

Herein, we performed a detailed analysis of the theoretical studies of the enzymatic ATP conversion to ADP or cAMP. Both of these reactions are initiated by the nucleophilic attack of an oxygen atom and lead to the cleavage of the bridging P–O bond. In both reactions an additional water molecule is required to transfer a proton from the nucleophile to the acceptor. Still, the mechanisms of the formation and cleavage of P–O bonds are considerably different. In adenylate cyclases it proceeds in a single step *via* associative mechanism, whereas in ATPases it occurs *via* dissociative mechanism. As an outlook, we demonstrate that the reaction mechanism can be rationalized *via* analysis of the dynamic behavior of the enzyme–substrate complex taking two examples belonging to systems with different mechanisms. For the ATPase the cleaving P–O bond is generally longer, thus being more prepared for the break. This approach should be developed and utilized for other systems to explain differences in reaction mechanisms.

The authors acknowledge financial support from the Russian Science Foundation, project 23-13-00011. The research is carried out using the equipment of the shared research facilities of HPC computing resources at Lomonosov Moscow State University.

References

- 1 M. Rigoulet, C. L. Bouchez, P. Paumard, S. Ransac, S. Cuvellier, S. Duvezin-Caubet, J. P. Mazat and A. Devin, *Biochim. Biophys. Acta, Bioenerg.*, 2020, **1861**, 148276.
- 2 M. Bonora, S. Paternani, A. Rimessi, E. De Marchi, J. M. Suski, A. Bononi, C. Giorgi, S. Marchi, S. Missiroli, F. Poletti, M. R. Wieckowski and P. Pinton, *Purinergic Signalling*, 2012, **8**, 343.
- 3 D. Petrović, K. Szeler and S. C. L. Kamerlin, *Chem. Commun.*, 2018, **54**, 3077.
- 4 I. Rayment, H. Holden, M. Whittaker, C. Yohn, M. Lorenz, K. Holmes and R. Milligan, *Science*, 1993, **261**, 58.
- 5 C. R. Bagshaw, J. F. Eccleston, F. Eckstein, R. S. Goody, H. Gutfreund and D. R. Trentham, *Biochem. J.*, 1974, **141**, 351.
- 6 D. R. Trentham, J. F. Eccleston and C. R. Bagshaw, *Q. Rev. Biophys.*, 1976, **9**, 217.
- 7 Z. Song, K. J. Parker, I. Enoh, H. Zhao and O. Olubajo, *Anal. Bioanal. Chem.*, 2009, **395**, 1453.
- 8 N. Okimoto, K. Yamanaka, J. Ueno, M. Hata, T. Hoshino and M. Tsuda, *Biophys. J.*, 2001, **81**, 2786.
- 9 G. Li and Q. Cui, *J. Phys. Chem. B*, 2004, **108**, 3342.
- 10 S. M. Schwarzel, J. C. Smith and S. Fischer, *Biochemistry*, 2006, **45**, 5830.
- 11 Y. Yang, H. Yu and Q. Cui, *J. Mol. Biol.*, 2008, **381**, 1407.
- 12 B. L. Grigorenko, A. V. Rogov, I. A. Topol, S. K. Burt, H. M. Martinez and A. V. Nemukhin, *Proc. Natl. Acad. Sci. USA*, 2007, **104**, 7057.
- 13 B. L. Grigorenko, I. A. Kaliman and A. V. Nemukhin, *J. Mol. Graph. Model.*, 2011, **31**, 1.
- 14 F. A. Kiani and S. Fischer, *J. Biol. Chem.*, 2013, **288**, 35569.
- 15 F. A. Kiani and S. Fischer, *Proc. Natl. Acad. Sci. USA*, 2014, **111**, E2947.
- 16 F. A. Kiani and S. Fischer, *Curr. Opin. Struct. Biol.*, 2015, **31**, 115.
- 17 T. Vasilevskaya, M. G. Khrenova, A. V. Nemukhin and W. Thiel, *Mendeleev Commun.*, 2016, **26**, 209.
- 18 A. Kulakova, S. Lushchekina, B. Grigorenko and A. Nemukhin, *J. Theor. Comput. Chem.*, 2015, **14**, 1550051.
- 19 H. Onishi, T. Ohki, N. Mochizuki and M. F. Morales, *Proc. Natl. Acad. Sci. USA*, 2002, **99**, 15339.
- 20 H. Onishi, N. Mochizuki and M. F. Morales, *Biochemistry*, 2004, **43**, 3757.
- 21 A. Málnási-Csizmadia, D. S. Pearson, M. Kovács, R. J. Woolley, M. A. Geeves and C. R. Bagshaw, *Biochemistry*, 2001, **40**, 12727.
- 22 J. Weber and A. E. Senior, *Biochim. Biophys. Acta, Bioenerg.*, 1997, **1319**, 19.
- 23 J. P. Abrahams, A. G. W. Leslie, R. Lutter and J. E. Walker, *Nature*, 1994, **370**, 621.
- 24 M. Dittrich, S. Hayashi and K. Schulten, *Biophys. J.*, 2003, **85**, 2253.
- 25 M. Dittrich, S. Hayashi and K. Schulten, *Biophys. J.*, 2004, **87**, 2954.
- 26 M. Dittrich and K. Schulten, *J. Bioenerg. Biomembr.*, 2005, **37**, 441.

27 M. K. al-Shawi, D. Parsonage and A. E. Senior, *J. Biol. Chem.*, 1989, **264**, 15376.

28 S. Hayashi, H. Ueno, A. R. Shaikh, M. Umemura, M. Kamiya, Y. Ito, M. Ikeguchi, Y. Komoriya, R. Iino and H. Noji, *J. Am. Chem. Soc.*, 2012, **134**, 8447.

29 R. Watanabe, R. Iino and H. Noji, *Nat. Chem. Biol.*, 2010, **6**, 814.

30 F. Martín-García, J. I. Mendieta-Moreno, I. Marcos-Alcalde, P. Gómez-Puertas and J. Mendieta, *Biochemistry*, 2013, **52**, 959.

31 S. A. Endow, *Eur. J. Biochem.*, 1999, **262**, 12.

32 J. C. Cochran and S. P. Gilbert, *Biochemistry*, 2005, **44**, 16633.

33 J. C. Cochran, T. C. Krzysiak and S. P. Gilbert, *Biochemistry*, 2006, **45**, 12334.

34 M. J. McGrath, I.-F. W. Kuo, S. Hayashi and S. Takada, *J. Am. Chem. Soc.*, 2013, **135**, 8908.

35 C. G. dos Remedios, D. Chhabra, M. Kekic, I. V. Dedova, M. Tsubakihara, D. A. Berry and N. J. Nosworthy, *Physiol. Rev.*, 2003, **83**, 433.

36 J. Akola and R. O. Jones, *J. Phys. Chem. B*, 2006, **110**, 8121.

37 H. Freedman, T. Laino and A. Curioni, *J. Chem. Theory Comput.*, 2012, **8**, 3373.

38 M. McCullagh, M. G. Saunders and G. A. Voth, *J. Am. Chem. Soc.*, 2014, **136**, 13053.

39 M. A. Rould, Q. Wan, P. B. Joel, S. Lowey and K. M. Trybus, *J. Biol. Chem.*, 2006, **281**, 31909.

40 L. Blanchoin and T. D. Pollard, *Biochemistry*, 2002, **41**, 597.

41 Y. Kanematsu, A. Narita, T. Oda, R. Koike, M. Ota, Y. Takano, K. Moritsugu, I. Fujiwara, K. Tanaka, H. Komatsu, T. Nagae, N. Watanabe, M. Iwasa, Y. Maéda and S. Takeda, *Proc. Natl. Acad. Sci. USA*, 2022, **119**, e2122641119.

42 K. F. Ostrom, J. E. LaVigne, T. F. Brust, R. Seifert, C. W. Dessauer, V. J. Watts and R. S. Ostrom, *Physiol. Rev.*, 2022, **102**, 815.

43 C. W. Dessauer and A. G. Gilman, *J. Biol. Chem.*, 1997, **272**, 27787.

44 J. J. G. Tesmer, R. K. Sunahara, R. A. Johnson, G. Gosselin, A. G. Gilman and S. R. Sprang, *Science*, 1999, **285**, 756.

45 S.-Z. Yan, Z.-H. Huang, R. S. Shaw and W.-J. Tang, *J. Biol. Chem.*, 1997, **272**, 12342.

46 Y. Liu, A. E. Ruoho, V. D. Rao and J. H. Hurley, *Proc. Natl. Acad. Sci. USA*, 1997, **94**, 13414.

47 L. Mones, W.-J. Tang and J. Florián, *Biochemistry*, 2013, **52**, 2672.

48 D. K. Hahn, J. R. Tusell, S. R. Sprang and X. Chu, *Biochemistry*, 2015, **54**, 6252.

49 G. E. Jara and L. Martínez, *J. Phys. Chem. B*, 2016, **120**, 6504.

50 B. Grigorenko, I. Polyakov and A. Nemukhin, *J. Phys. Chem. B*, 2020, **124**, 451.

51 M. G. Khrenova, A. M. Kulakova and A. V. Nemukhin, *J. Chem. Inf. Model.*, 2021, **61**, 1215.

52 A. M. Kulakova, T. I. Mulashkina, A. V. Nemukhin and M. G. Khrenova, *Russ. Chem. Bull.*, 2022, **71**, 921.

53 I. V. Polyakov, M. G. Khrenova, B. L. Grigorenko and A. V. Nemukhin, *Mendeleev Commun.*, 2022, **32**, 739.

54 M. G. Khrenova, V. G. Tsirelson and A. V. Nemukhin, *Phys. Chem. Chem. Phys.*, 2020, **22**, 19069.

55 M. G. Khrenova, A. V. Nemukhin and V. G. Tsirelson, *Mendeleev Commun.*, 2020, **30**, 583.

56 M. G. Khrenova, B. L. Grigorenko and A. V. Nemukhin, *ACS Catal.*, 2021, **11**, 8985.

57 C. A. Smith and I. Rayment, *Biochemistry*, 1996, **35**, 5404.

Received: 20th July 2023; Com. 23/7210